Volume 13 Number 20 1985 Nucleic Acids Research

Evidence for the translational attenuation model: ribosome-binding studies and structural analysis with an *in vitro* run-off transcript of *ermC*

C.S.Narayanan and D.Dubnau

Department of Microbiology, The Public Health Research Institute of the City of New York, 455 First Avenue, New York, NY 10016, USA

Received 24 July 1985; Revised and Accepted 16 September 1985

ABSTRACT

Several features of the translational attenuation model of ermC regulation were tested. This model predicts two possible secondary structures for the leader of the ermC transcript and requires that the leader contains two Shine-Dalgarno (SD) sequences. The ribosome binding site for a leader peptide (SD1) is predicted to be accessible, whereas that for the rRNA methylase protein that confers erythromycin (Em) resistance (SD2) is sequestered by base pairing. The model suggests that in the presence of inducer (Em), a ribosome stalls while translating the peptide, altering the mRNA conformation, thereby exposing SD2. The results of our ribosome binding studies demonstrate that SD1 is exposed and binds to ribosomes, whereas SD2 is unavailable. Also, the secondary structure of the 5' region of the ermC transcript was analyzed using methidium propyl-EDTA·Fe(II), T1 nuclease, and nucleases from cobra venom and mung bean sprouts as structure probes. Our results support the previously proposed model for folding of ermC mRNA, and demonstrate that SD1 is single-stranded, while SD2 and its neighboring sequences are largely base paired, consistent with the ribosome-binding results.

INTRODUCTION

Macrolide-lincosamide-streptogramin B (MLS) antibiotics bind to the large ribosomal subunit and inhibit protein synthesis (1). ermC confers resistance to these antibiotics, and specifies a 29,000 Dalton rRNA methylase (2, 3). ermC was discovered on the Staphylococcus aureus plasmid pE194 (3a), which was subsequently introduced by transformation into Bacillus subtilis (4). The rRNA methylase dimethylates a specific adenine residue in 23 S rRNA, resulting in ribosomes with lowered affinity for the MLS antibiotics (4, 5). Other MLS-resistance determinants had previously been shown to act in this way (6,7,8). In the presence of erythromycin (Em) at subinhibitory concentrations, ermC expression and consequently resistance are induced (2,3,4). Induction of ermC methylase production is posttranscriptionally controlled (5). A model has been proposed to explain how an inhibitor of protein synthesis can induce the synthesis of a protein. The proposed mechanism has been termed translational attenuation (9, 10).

Sequence analysis of ermC indicated the presence of a 140 base leader sequence between the promoter and the initiation codon for the methylase (9, 10). The 5' region of the transcript contains two regions rich in G residues which resemble ribosome binding site sequences (referred to as Shine-Dalgarno sequences [SD] (11)): a GGAGG at position 10 (SD1),and a GAGGG at position 131 (SD2). These sequences exhibit substantial complementarity to the 3' end of 16 S rRNA from B. subtilis. Following SD1 is an open reading frame sufficient to encode a 19 amino acid peptide. The 5' region of ermC mRNA is predicted to assume one or both of two possible secondary structures (Fig. 1) with the following features: SD2 is partially base paired, the initiation codon for the methylase is completely sequestered, and the ribosome binding site for the putative leader peptide is in a single-stranded configuration. The translational attenuation model postulates that during induction an Em-bound ribosome stalls near the C terminus of the leader peptide, thereby unmasking the ribosome binding site for methylase protein. Translation of the methylase protein would now be initiated by an Em-free, or already methylated, ribosome. Both postulated structures shown in Fig. 1 are compatible with this model. Unmasking of the ribosome binding site for methylase synthesis would occur directly in structure C and by a spontaneous refolding process in structure B. Structure C is predicted thermodynamically to be more stable than B at equilibrium. Analyses of deletion, substitution and duplication mutants support the translational attenuation model (14, 15, 16). However, several initial predictions of the model have remained untested. These include the secondary structure of the ermC transcript leader region that was predicted from the primary sequence, as well as the accessibility of SD1 and the unavailability of SD2 for ribosome binding. We have analyzed the interaction of ribosomes with the leader region of the ermC transcript and we have probed the structure of the transcript. Our results provide further support for the model.

MATERIALS AND METHODS

Materials. Ribonucleoside triphosphates were purchased from Sigma Chemical Co. E. coli RNA polymerase holoenzyme and cobra venom ribonuclease (CVR) were generous gifts of J.S. Krakow (Hunter College, New York), and J. N. Vournakis (Syracuse, N.Y.), respectively. Methidiumpropyl-EDTA (MPE) was a generous gift of P. Dervan (California Institute of Technology). [γ^{32}P]ATP (5,000 Ci/mmol) was from Amersham. [α^{32}P]ATP (25 Ci/mmol) was from ICN. Calf intestinal alkaline phosphatase (CIAP), T4 polynucleotide kinase, and T1

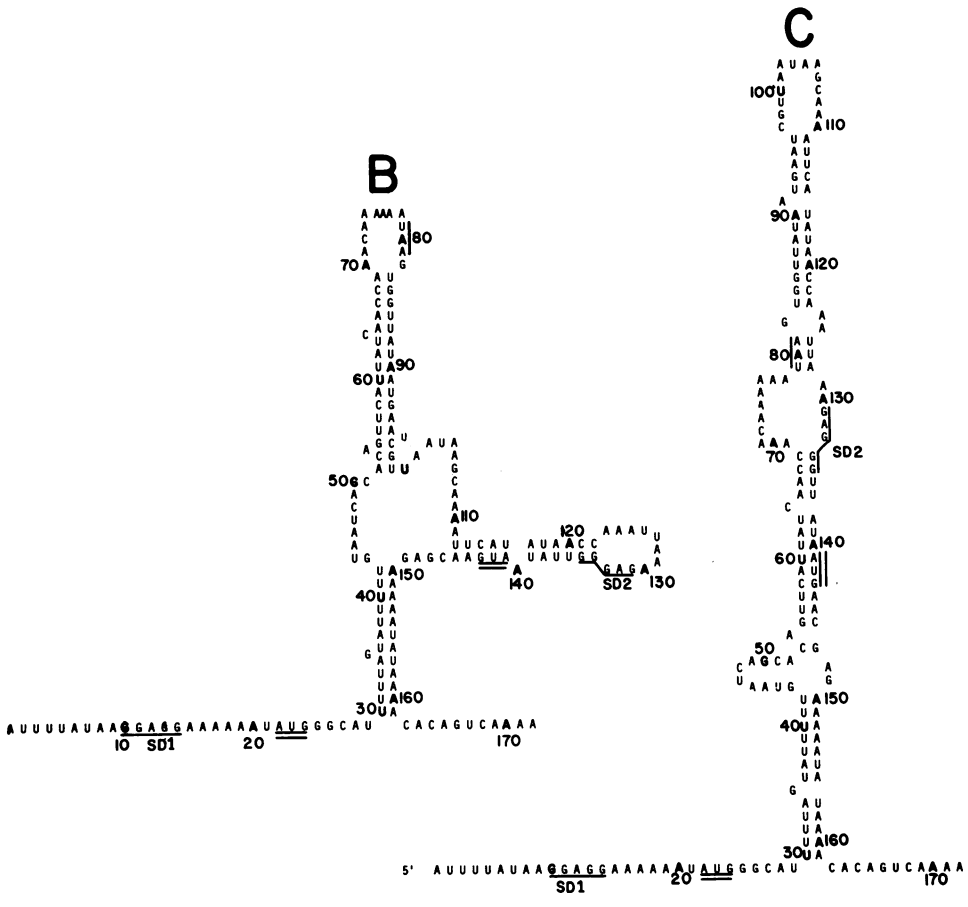

FIG. 1. Predicted secondary structures of the leader region of the ermC mRNA. (Structure A [not shown] is a proposed active configuration [9]). The positions of SD1 and SD2 and the leader peptide termination codon are indicated by single lines, and the start codons for the leader peptide and the rRNA methylase by double lines. ΔG values (-38.0 Kcal for B and -43.2 Kcal for C) were calculated using the method of Salser (12) as modified by Cech et al.(13). Structures B and C have been slightly modified from previous presentations (9) to minimize ΔG values. Specifically, an AU pair is omitted from the base of B and C, and the pairing near the central loop in B has been readjusted.

nuclease were from Boehringer. Mung bean nuclease (MBN) was from PL-Biochemicals. Double distilled water was used throughout. All the buffers and solutions were filter sterilized and autoclaved. The buffers were prepared using diethyl pyrocarbonate (DEP) treated H_2O. DEP was added to 10 mM, the solution was stirred at 4°C for 8 h and then autoclaved. Acrylamide gels were prepared in 7 M urea and 1 x TBE buffer.

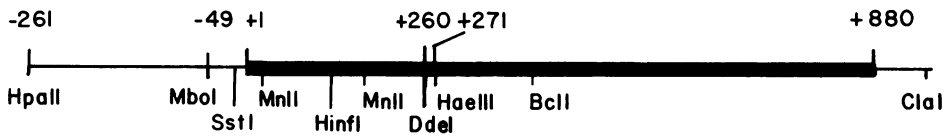

FIG. 2. Partial restriction map of the ermC gene. The HpaII-ClaI fragment of pE194, which contains ermC, is shown, together with some relevant restriction sites. +1 is the transcriptional initiation site of ermC. The sizes of the run-off transcripts which terminate at the DdeI and HaeIII sites are 260 and 271 bases, respectively. The complete ermC transcript (~880 bases) is indicated relative to the initiation site. The MnlI sites (GAGG) mark the positions of SD1 and SD2.

Buffers. S1 nuclease - 40 mM Na acetate (pH 4.5), 10 mM $ZnSO_4$, 0.2 M NaCl; MBN - 30 mM Na acetate (pH 4.5), 50 mM NaCl, 1 mM $ZnCl_2$; T1 nuclease- 10 mM Na acetate (pH 5), 0.2 M NaCl, 10 mM $MgCl_2$; CVR - 10 mM Tris-HCl (pH 7.5), 2 mM $MgCl_2$, 0.2 M NaCl; ribosome binding buffer - 10 mM Tris-HCl (pH 7.4), 10 mM Mg acetate, 60 mM NH_4Cl, 6 mM β-mercaptoethanol; kinase buffer - 50 mM Tris-HCl (pH 9), 10 mM $MgCl_2$, 5 mM DTT, 0.1 mM EDTA; TBE - 90 mM Tris-OH, 90 mM boric acid, 2.5 mM EDTA. Acrylamide stock solution contained 38% acrylamide and 2% bis-acrylamide.

Plasmid DNA. High copy number derivatives of pE194 (pBD285 and pBD15) were used as sources of DNA. The B. subtilis BD170 cultures containing these plasmids were grown to stationary phase at 33°C, and the plasmid DNA was purified as described earlier (17).

Synthesis of run-off transcripts. A 520 base pair DNA fragment containing the ermC promoter was isolated from a HpaII-DdeI digest of pBD285 or pBD15 and used as template (Fig. 2). The reaction condition used for transcription was as follows: 80 mM Tris-HCl (pH 7.8), 10% glycerol, 0.1 mM EDTA, 0.1 mM DTT, 150 mM KCl, 10 mM $MgCl_2$, 40 μg/ml BSA, 1 to 4 μg DNA template, 1 μg RNA polymerase, and 500 μM each of the ribonucleoside triphosphates. The reaction was carried out at 37°C for 30 min in a 25 μl volume. The DNA-RNA polymerase complex was allowed to form at 37°C for 2 min prior to the addition of the nucleoside triphosphate mix.

End-labeling of the transcript. Following transcription, the reaction mix was extracted with an equal volume of phenol-$CHCl_3$ (1:1). A stock solution (half the volume of aqueous phase) of 8 M NH_4 acetate, 10 mM EDTA was added to the aqueous phase. Three volumes of ethanol were added and the solution was chilled in a dry ice-ethanol bath for 10 min. The precipitate was collected by centrifugation. The nucleic acids were redissolved in 90 μl water, brought to 10 mM Tris-HCl (pH 7.5) and treated with 0.1 u of CIAP at

37°C for 30 min. Following phenol-$CHCl_3$ extraction and ethanol precipitation, the nucleic acids were 5' end-labeled with 0.1 to 0.5 u of kinase in 100 µl kinase buffer containing 5 µl [γ^{32}P]ATP (50 µCi). Following incubation at 37°C for 30 min, the end-labeled nucleic acids were again phenol-$CHCl_3$ extracted, ethanol precipitated, dissolved in deionized formamide and electrophoresed on a 5% acrylamide-urea gel (16 x 14 x 0.15 cm) for 2.5 h at a constant voltage of 100 volts in TBE buffer. Since the template contains 260 bases upstream from the ermC promoter, the end-labeled run-off transcript was easily separated from the end-labeled template by electrophoresis. After autoradiography at room temperature for 3 to 5 min the transcript band was excised from the gel and the labeled transcript was electroeluted as follows: The gel piece was placed in a dialysis bag containing 0.1 x TBE and the transcript was electroeluted in a chamber (18 x 14 x 4 cm) containing 0.1 x TBE, at 200-300 volts for 1 h at 4°C. The eluted transcript was ethanol precipitated, dissolved in water and stored at 4°C (18). In a typical labeling experiment transcript containing 4 to 5 x 10^5 cpm was obtained.

Ribosome binding studies. High salt-washed ribosomes were purified from B. subtilis BD170 according to the procedure described by Guha and Szulmajster (19). 0.1 to 1 A_{260} O.D. units of ribosomes were incubated in 5 µl ribosome binding buffer together with 5 to 15,000 cpm (Cerenkov) of [γ^{32}P]ATP end-labeled transcript, and 0.2 mM GTP at 37°C for 10 min. After cooling the reaction mix to room temperature, the indicated amounts of T1 or MBN were added, and incubation was continued at room temperature. After 30 min, 5 µl formamide dye was added, and 5 µl was analyzed by polyacrylamide-urea gel electrophoresis, as described below. In control experiments the ribosomes were omitted, and 2.5 µg tRNA was included instead.

Ribosome interactions were also studied essentially as described by Steitz (20). 30,000 to 40,000 cpm of [α^{32}P] or [γ^{32}P]ATP-labeled run-off transcript was incubated at 37°C for 10 min with 1 to 5 A_{260} O.D. units of ribosomes in ribosome binding buffer containing 0.2 mM GTP, with and without 0.5 mM ATP, 5 µg of f-met tRNA, 20 µg of E. coli MRE 600 tRNA (final volume 20 µl). Different amounts of RNase T1 or RNase A were added, and the mixture was incubated at room temperature for 20 min. It was then layered on a 5 ml, 5 to 20% linear sucrose gradient in ribosome binding buffer (minus β-mercaptoethanol) and centrifuged for 2 h at 39,000 rpm in an SW 50 rotor (Beckman) at 4°C. Fractions of 0.5 ml were collected and those containing ribosomes were pooled, phenol-$CHCl_3$ extracted, ethanol precipitated and dissolved in 10 µl T1 nuclease buffer containing 7 M urea. 5 µl of this was loaded on a 15%

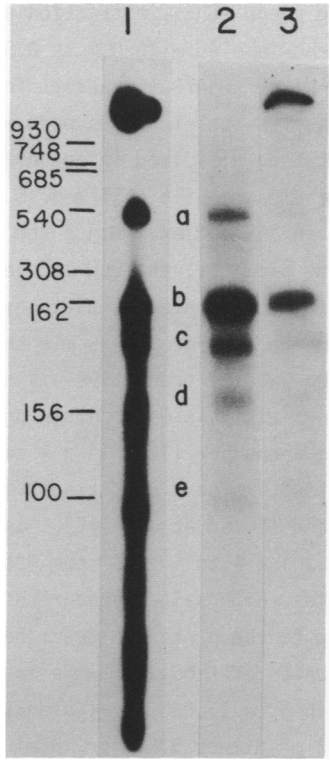

FIG. 3. Transcription with the HpaII-DdeI fragment as template. Lane 1, end-labeling following transcription was carried out using T4 poly-nucleotide kinase as described in Materials and Methods, with 3 µg DNA template. The labeled nucleic acids were dissolved in 30 µl deionized formamide and electrophoresed on a 5% polyacrylamide-urea gel. Lane 2, transcription was carried out using [α^{32}P]ATP as described in Materials and Methods, followed by electrophoresis on a 5% polyacrylamide-urea gel. Lane 3, transcription as in lane 2, but using [γ^{32}P]ATP. a: DNA template; b: major transcript; c, d, and e: minor transcripts. The positions of DNA marker fragments (5' end-labeled MboI-DdeI digest of pBD15 DNA) and their sizes in base pairs, are shown.

polyacrylamide-urea gel as described below. The other 5 µl was treated with 20 to 50 u of T1 nuclease, at 55°C for 10 min before loading on a 15% polyacrylamide-urea gel.

RNA sequencing and structure probing. RNA sequencing was carried out enzymatically, essentially as described by Vournakis et al. (18). Structure probing experiments were carried out as follows: the labeled transcript (5 to 15,000 cpm, determined by Cerenkov counting) together with 2.5 or 3.3 µg tRNA was preincubated in the appropriate nuclease buffer at 37°C for 10 min and

then cooled to room temperature. Following the addition of the indicated amount of nuclease, the mix (total volume of 5 µl) was incubated at room temperature for 30 min. Five µl of formamide containing 0.001% Bromophenol Blue and Xylene Cyanol was added, and 5 µl of this was loaded on polyacrylamide urea sequencing gels (60 x 28 x 0.04 cm, or 45 x 38 x 0.04 cm) and electrophoresed in TBE buffer at 2500 to 3000 volts, maintaining a gel temperature of 45°C to 50°C. In various experiments, 10-20% polyacrylamide gels were used, as indicated. Formamide ladders were obtained by boiling labeled transcript (5 to 15,000 cpm) and 2.5 µg tRNA in 10 µl formamide for 30 min (21). Structure probing with MPE was carried out in CVR buffer according to the procedures described by Vary and Vournakis (22).

RESULTS

Fig. 3 (lane 1) shows the result obtained when the run-off products of an *in vitro* transcription reaction, carried out as described in Methods, were 5'-end-labeled. Fig. 3 also shows the result of transcription carried out in the presence of [α^{32}P]ATP (lane 2) or [γ^{32}P]ATP (lane 3). Band *a* contains the DNA template plus a different conformational form of the major transcript (not shown). Band *b* is the major transcript. Bands *c*, *d*, and *e* are minor transcripts. Since the minor bands are identical in experiments using α or γ ATP in the transcription mix, they are unlikely to be degradation products. Labeling transcript using T4 kinase as described above involves a single polyacrylamide gel extraction compared to the two required in the conventional end-labeling of transcript which has been uniformly labeled at low specific activity (23). This tends to minimize RNA degradation.

Enzymatic sequence analysis of band *b* (not shown) indicated that it was the expected *ermC* transcript, confirming that *E. coli* RNA polymerase initiates accurately at the *ermC* start site. S1 nuclease mapping had suggested that transcription initiates at one of two tandem A residues (9). Our RNA sequencing analysis suggested strongly that the downstream A is the initiating nucleotide. The numbering system used below is based on this finding. Identical sequencing results were obtained with transcriptionally end-labeled or kinase end-labeled fragments, or with transcript obtained using *Mbo*I-*Dde*I, *Hpa*II-*Dde*I, or *Hpa*II-*Hae*III fragments as template. These fragments yield run-off transcripts containing 260, 260, and 271 bases, respectively, but initiate at the same residue. Run-off transcript was also obtained using plasmid DNA, linearized at the unique *Hae*III site, as template.

In our polyacrylamide-urea gels (see Fig. 4, lane 1) limited degradation

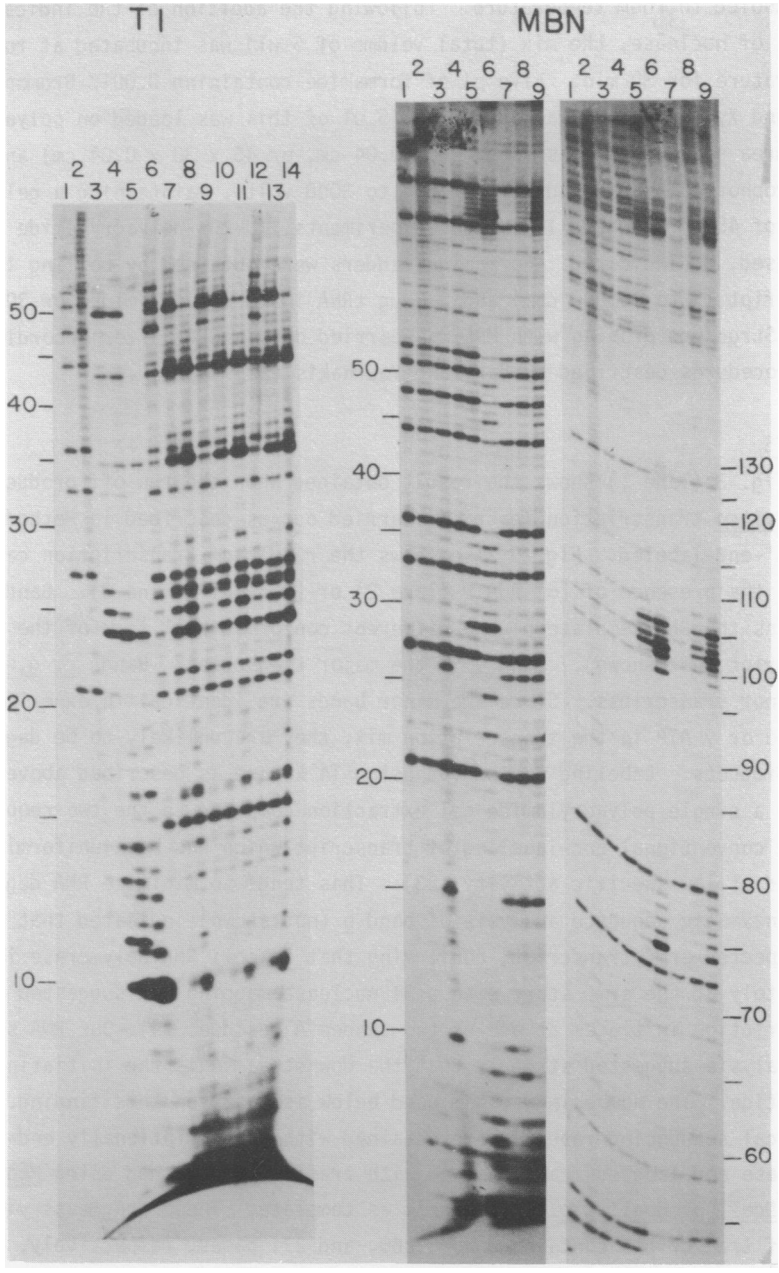

FIG. 4. Ribosome protection study. These studies were carried out as described in Materials and Methods. T1 nuclease: 1, labeled transcript (no enzyme or ribosomes); 2, formamide ladder; 3-5, no ribosomes; 6-8, 1 A_{260}

O.D. unit of ribosomes; 9-11, 1 O.D. unit of ribosomes + 2.5 µg f-met tRNA; 12-14, 1 O.D. unit of ribosomes + 2.5 µg E. coli MRE600 tRNA. The amount of T1 nuclease used was as follows: 0.01 u for 3, 6, 9, 12; 0.1 u for 4, 7, 10 and 13; and 1 u for 5, 8, 11, and 14. MBN: The panels on the left and right represent second and first loadings, respectively. 1, labeled transcript (no enzyme or ribosomes); 2, formamide ladder; 3, labeled transcript with 1 O.D. unit of ribosomes; 4, 5, 6, labeled transcript with 2.5 µg tRNA in ribosome binding buffer digested with 0.1, 1, 10 u of MBN, respectively; 7, 8, 9, labeled transcript with 2 O.D. units of ribosomes digested with 0.1, 1, 10 u of MBN, respectively.

of the transcript was always noted in the absence of added nucleases. Despite rigorous precautions, this degradation could not be eliminated. However, it was found to be specific, occurring 5' to those pyrimidine residues which are followed by A residues. A similar cleavage specificity in "untreated" samples has been reported for E. coli 16 S rRNA (24). Since this pattern of degradation was highly reproducible, it was helpful in assigning nuclease-sensitive sites in the structure probing experiments.

Ribosome protection study. Figure 4 shows the results obtained in ribosome protection experiments using [γ^{32}P]ATP end-labeled transcript. Lanes 3-5 show cleavage by T1 nuclease in the absence of protecting ribosomes. When excessive T1 concentrations were used (lanes 4 and 5), extra bands with faster migration were observed, possibly due to the formation of cyclic 2',3' phosphate products. However, when a lower amount of T1 nuclease was used (lane 3), the G residues at positions 10, 11, 13, and 14 corresponding to the putative ribosome binding site of the leader peptide, are seen to be sensitive to cleavage. When ribosomes are present (lanes 6-14) these positions are protected from cleavage. The G residues at 24, 25, and possibly 26 also show decreased sensitivity to T1 nuclease in the presence of ribosomes: approximately 10 times more T1 nuclease was required in the presence of ribosomes in order to obtain the same band intensity as in the absence of ribosomes. The G residues at positions 35, 43, or 50 showed no decrease in sensitivity to T1 nuclease in the presence of ribosomes. The increased intensity of the bands corresponding to these positions could be due to the accumulation of fragments because of the decreased accessibility of other G residues to T1 nuclease in the presence of ribosomes. The sensitivity of G residues at positions 82, 98, and 106 remained unchanged in the presence of ribosomes (not shown). In addition, the T1 nuclease-sensitivity of the G residue at 131, located within SD2, was unaffected by the presence of ribosomes (not shown). Fig. 4 also shows ribosome protection studies carried out with MBN. Nucleotides 17 through 20 and 29 through 35,which are sensitive to MBN in the absence of

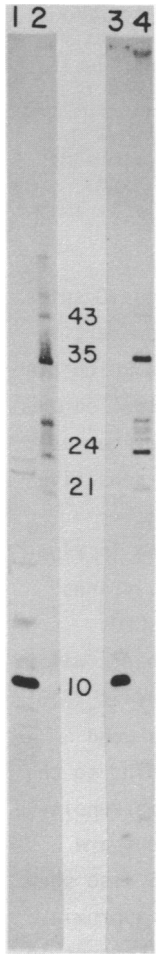

FIG. 5. Ribosome protection study. 2, 4, protection of fragments by ribosomes against T1 digestion; 1, 3, the fragments shown in lanes 2 and 4 were treated secondarily with T1 nuclease under denaturing conditions. In lanes 1 and 2, [α^{32}P]ATP-labeled transcript was used, and in lanes 3 and 4 [γ^{32}P]ATP-labeled transcript was used. The sizes of several relevant fragments are given in bases.

ribosomes, become less sensitive in their presence. This is very apparent at position 29 where a strong band is obtained only in the absence of ribosomes. Nucleotides 46-50, 74-78, and 101-105 show no decrease in MBN sensitivity in the presence of ribosomes. The cleavages by MBN at residues 126-130, including the relatively strong cleavage at position 128, were not decreased in the presence of ribosomes, further suggesting that binding does not occur in the neighborhood of SD2.

Ribosome-mRNA interactions were also studied using [α^{32}P]ATP-labeled as well as [γ^{32}P]ATP end-labeled transcripts by incubation under the conditions described in Materials and Methods, followed by analysis on 5-20% sucrose gradients. Salt-washed and unwashed B. subtilis ribosomes were compared, in

TABLE 1. Summary of Cleavages by Structure Probes

Probe	Sensitive positions*
T1 nuclease	10-11, 13-14, 24-26, 35, 43, 50, 82, 98, 106, 131, (149), (166)
MBN	2-10, 13, 15-20, (21), 22-23, (24-28), 29, (30-44), 45-47, (48), 49-50, 74-78, 100-108, 126-131
MPE	15-23, 28-45, 55-65, 80-81, 83-84, 88-93, 114-121
CVR	13, 15, 17-23, 29-30, 38-42, 67-69, 93, 96-98, 117-118, 121-123, 142, 145, 156-158

*The numbering system and positions of SD1 (10-14) and SD2 (131-135) are shown in Fig. 1. Numbers in parentheses refer to weakly cleaved positions.

the presence and absence of the following additions: f-met tRNA, tRNA, ATP, and GTP. Using washed ribosomes, 34% of the uniformly labeled transcript was bound in the presence of the additives, and 31% in their absence. When unwashed ribosomes were used, these values fell to 24% and 17%, respectively. These results are consistent with the previous findings of McLaughlin et al. (25), that initiation factors are not absolutely required for binding of B. subtilis mRNA to ribosomes. When the bound transcript was digested with ribonucleases prior to sucrose gradient centrifugation, the percentage of the starting cpm bound to salt-washed ribosomes decreased from 34% to 6% when RNase A was used, and to 9% with RNase T1.

The T1 RNase and RNase A-protected fragments bound by salt-washed B. subtilis ribosomes in the presence of the additives were analyzed on polyacrylamide gels (Fig. 5). The smallest major fragment protected by ribosomes against T1 nuclease is 24 nucleotides in length and the largest major fragment is 35 nucleotides long. The 21 base fragment seen in Fig. 5 (lanes 2 and 4) is probably a degradation product, since no 21 base T1 fragment can be derived from the run-off transcript sequence. The minor 43 base fragment visible in Fig. 5 (lanes 2 and 4) may be due to partial protection extending to the G at position 43. The patterns of ribosome-protected fragments were identical when [α^{32}P]ATP or [γ^{32}P]ATP-labeled transcripts were used. This demonstrates

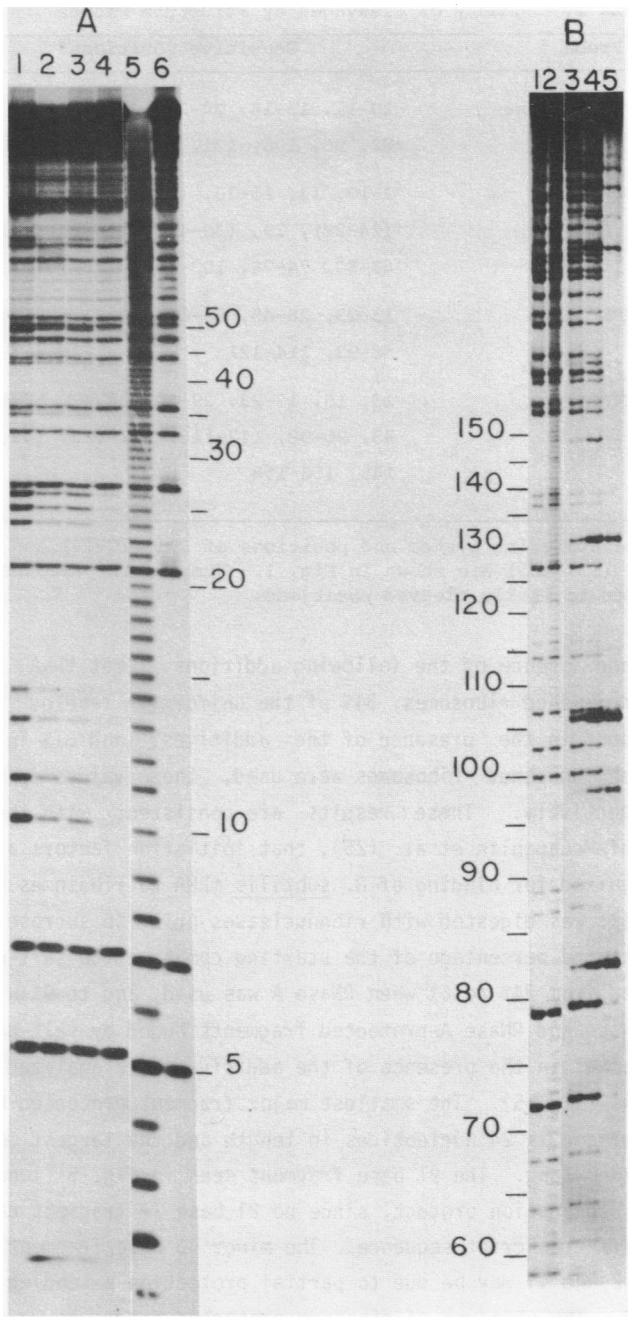
A
1 2 3 4 5 6
50
40
30
20
10
5
B
1 2 3 4 5
150
140
130
120
110
100
90
80
70
60

clearly that ribosome binding is at the 5' end and not in the interior of the transcript. Secondary digestion of the protected fragments by T1 nuclease after removal of the bound ribosomes, yielded a major 10 base fragment from both [α^{32}P]ATP and [γ^{32}P]ATP-labeled transcripts. This fragment can only be obtained from the [γ^{32}P]ATP-labeled transcript by a T1 nuclease cleavage at position G10. Similar studies carried out using RNase A during the primary digestion suggested that at least 15 to 20 nucleotides are protected by ribosomes (not shown). Our results clearly demonstrate that a segment of ermC transcript extending from the 5' terminus at least to position 35 and possibly to residue 43 is protected by ribosome binding. This includes the SD1 sequence, as predicted by the ermC regulation model. Our results also demonstrate an absence of ribosome binding to SD2. For instance, protection of SD2 should result in T1 nuclease fragments 37, 41, or 43 residues in length (see Fig. 1). No major bands of these lengths are visible in lane 2. More telling, secondary cutting of these fragments with T1 nuclease would yield bands of 4, 8, and 25 residues. These are absent from lane 1. Taken as a whole, our findings agree well with results from the E. coli systems where 25 to 40 nucleotides are protected by ribosomes (26).

Structure-probing with T1 nuclease. The results obtained using T1 nuclease are shown in Fig. 6 and summarized in Table 1. The G nucleotides at positions 55, 84, 85, 93, 133, 134, 135, 143, and 147 are not cleaved by T1 and are therefore presumably base paired. These results are summarized in Fig. 9 and agree with the proposed structure C. However, G 133 and 149 are predicted to be unpaired, while our results show that G 133 is not available and G 149 is only slightly available for T1 nuclease cleavage. These nucleotides are near the 3' end of unpaired loops, and such nucleotides have been previously reported to be relatively inaccessible to both T1 and S1 nucleases (27).

Structure probing with MBN. Results obtained with partial digestions using MBN are shown in Fig. 7 and summarized in Table 1. Residues 2-10, 13, and a stretch from residue 15 through 50 are cleaved to varying extents. This is all in agreement with the structures shown in Fig. 1, except that positions

FIG. 6. Structure analysis of the ermC transcript: T1 nuclease studies. Structure probing experiments were carried out as described in Materials and Methods using 20% (panel A) or 10% (panel B) polyacrylamide gel. End-labeled RNA mixed with 3.3 µg tRNA (A) or 2.5 µg tRNA (B) was digested with 0.025 u T1 for 1' and 5' (lanes 4 and 3) or 0.1 u T1 for 1' and 5' (lanes 2 and 1). In panel B the digestion was carried out for 30' with 0.01, 0.1 or 1 u T1 (lanes 3, 4, and 5). Controls with no enzyme are shown in lanes 6(A) and 1(B), and formamide ladders are in lanes 5(A) and 2(B).

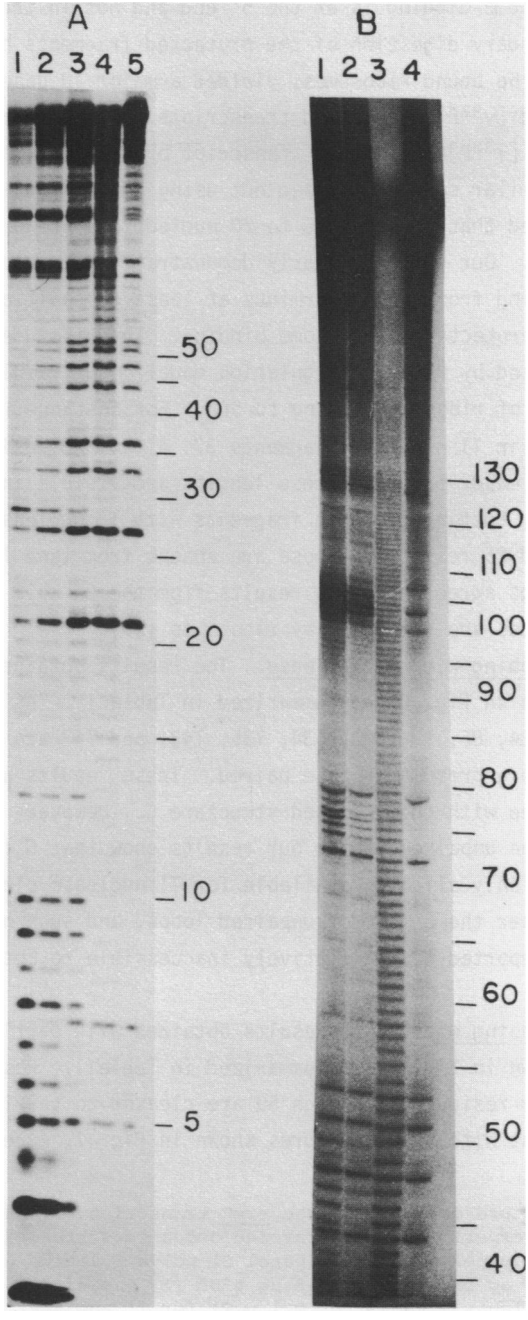
A
1 2 3 4 5
50
40
30
20
10
5
B
1 2 3 4
130
120
110
100
90
80
70
60
50
40

30-42 are predicted to be base paired. However, these are entirely AU pairs and might reasonably be expected to "breathe". Additional cleavages occur at positions 74-78, 100-108, and 126-131. These agree with the structures in Fig. 1, except that residues 126-128 are base-paired in structure C. These, however, are AU pairs, flanked by loops and would probably be unstable. Beyond approximately residue 135 we cannot reliably read our MBN gels.

Structure probing with MPE. MPE·Fe(II) cleaves base stacked regions of both DNA and RNA after intercalation (22, 28). Although some cleavage occurs at all residues, MPE·Fe(II) cleaves more strongly at base stacked positions. Fig. 8A (lanes 4-6) and 8B (lanes 1 and 2) show our results with this probe. These results are summarized in Table 1. Beyond residue 123, our gels were not reliably readable. Positions 15-23 are predicted to be single-stranded by the structures in Fig. 1, and most of these residues were observed to be susceptible to MBN (Fig. 7). Residues G10, G11, G13 and G14 were cleaved by T1 nuclease (Fig. 6). These apparent contradictions may be resolved by postulating an alternative structure in which the A and U residues 15-23, sometimes pair with the A and U residues between positions 30 and 42, imparting a partially double-strand character to all of these residues, as observed. The other MPE·Fe(II) sensitive positions are in accord with Fig. 1.

CVR studies. Our results with the double-strand specific probe CVR are shown in Fig. 8A (lanes 1-3), 8B (lanes 3, 4), and 8C (lane 3) and are summarized in Table 1. The double-strand assignments based on CVR cleavage are in accord with Fig. 1 with the following exceptions. Residue G13 is predicted to be single-stranded. We can offer no specific explanation for this discrepancy other than the possibility that G13 is involved in a tertiary interaction. However, the cleavage at G13 by MBN and T1 nuclease (see above) supports its essentially single-stranded character. Residues 15-23 were found to have partial double-strand character based on the MBN, T1 nuclease and MPE·Fe(II) studies described above. The CVR results are in accord and may be explained by the alternative structure already suggested. Residues 97 and 98 are predicted to be single-stranded by structure C and 123 by structure B. However, these residues would occur within single-strand segments immediately 3' to a base paired stem. Such residues have been reported to be CVR sensitive by J. Vournakis (personal communication).

FIG. 7. Structure analysis of the ermC transcript: MBN studies. End-labeled RNA mixed with 3.3 µg tRNA was digested with 0.05 u MBN for 1', 5' and 12' (lanes 3, 2 and 1 of A) or 2' and 7' (lanes 2 and 1 of B). Lanes 5(A) and 4(B) show untreated controls and 4(A) and 3(B) show formamide ladders.

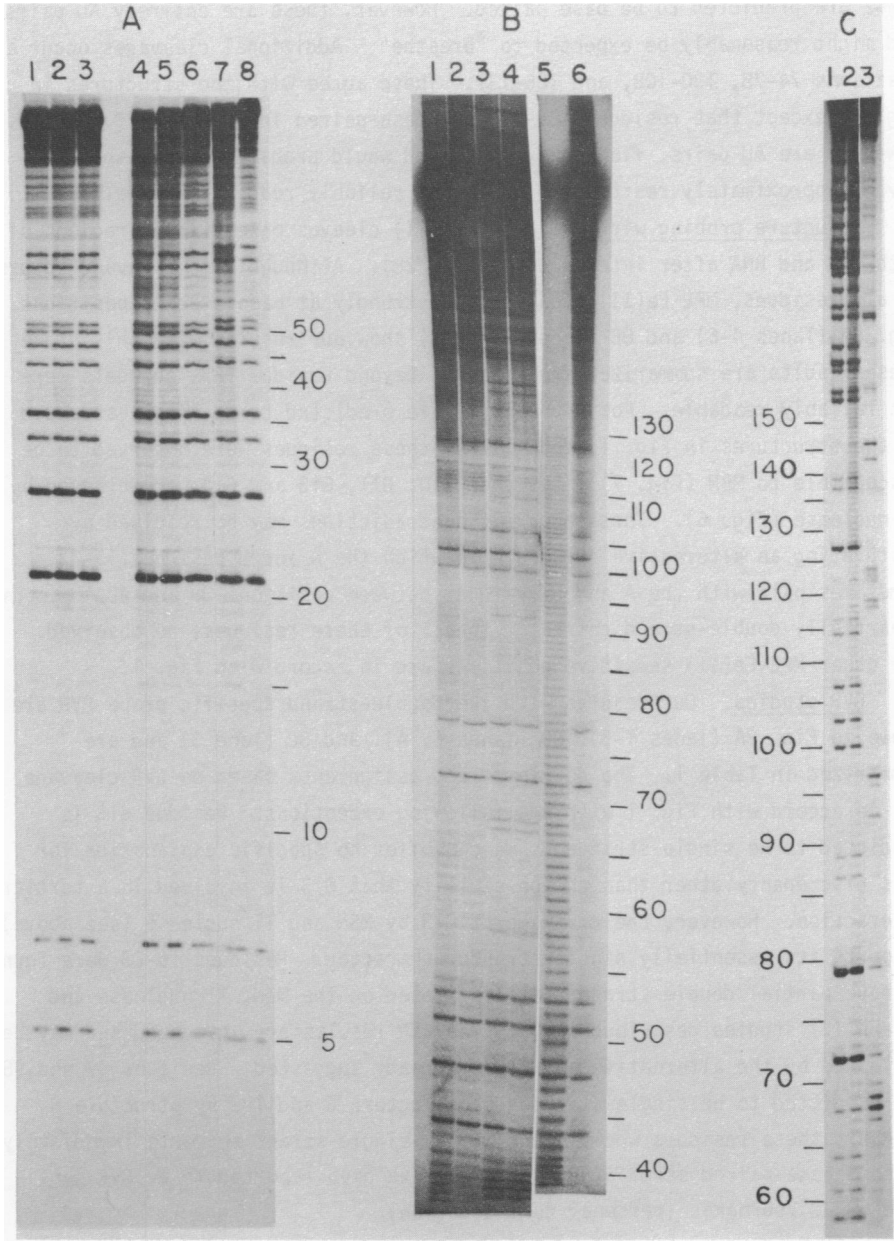

FIG. 8. Structure analysis of the ermC transcript: CVR and MPE·Fe(II) studies. Probing with MPE·Fe(II) was carried out according to the procedure described by Vary and Vournakis (22). End-labeled RNA mixed with 3.3 µg tRNA was preincubated in CVR buffer with 0.02 mM MPE and 0.02 mM ferrous ammonium sulfate (freshly made) at 37°C for 5'. Freshly prepared DTT was added to

5 mM (the reaction volume is 5 µl). Incubation was at room temperature for 1' and 4' (lanes 2 and 1 of B) or for 1', 3' and 6' (lanes 6, 5 and 4 of A). For CVR digestions, end-labeled RNA mixed with 3.3 µg tRNA (A and B) or 2.5 µg tRNA (C) was incubated with 1 µl of CVR (1:200 dilution of stock CVR) at room temperature for 1', 5' and 12' (lanes 3, 2, 1 or A) or 2' and 7' (lanes 4 and 3 of B) or 30' (lane 3 of C). Untreated controls are shown in lanes 8(A), 6(B), and 1(C) and formamide ladders are in 7(A), 5(B) and 2(C). Panels A and B are 20% and panel C is a 10% polyacrylamide gel.

DISCUSSION

The translational attenuation model was proposed to explain the regulation of synthesis of the MLS-specific rRNA methylase. According to this model, an Em-bound ribosome stalls during translation of the leader peptide. This causes isomerization of the mRNA structure permitting access of an Em-free ribosome to the ribosome binding site for the methylase protein. The model requires the presence of two ribosome binding sites in the inactive *ermC* transcript, one for the leader peptide that is usually free to bind ribosomes (SD1) and the other for the methylase protein that is normally sequestered by base-pairing (SD2). Two inactive secondary structures that satisfied the above requirements were proposed for the leader region of the *ermC* transcript, one predicted to be more stable than the other. Both structures are entirely consistent with the translational attenuation model (14). Our present results confirm an essential feature of the model: SD1 is available for ribosome binding, and SD2 is not.

SD1 (5'-AAGGAGG) is highly complementary to the 3' proximal sequence of *B. subtilis* 16 S rRNA (3'-UUCCUCC) (29), and base pairing is probably sufficient to explain the observed resistance of these residues to attack by MBN and T1 in the presence of ribosomes. Other residues in the neighborhood of SD1 may not base pair with rRNA, but may be protected from nuclease attack by other types of close contact with the ribosome. The T1, MBN and RNase A protection experiments taken together suggest that 35-43 residues, beginning at the 5' terminus of the *ermC* transcript and including SD1, can be found in close contact with ribosomes. We conclude, then, that these sequences constitute a ribosome-binding site preceding the putative leader peptide codons. This is consistent with our prediction, and with other data showing that SD1 is required for *ermC* induction (14), as is translation of the leader peptide coding sequence (16). The present results are also consistent with the prediction that the ribosome binding site for the methylase protein (SD2) is sequestered by base-pairing since no protection of SD2 by ribosomes was observed.

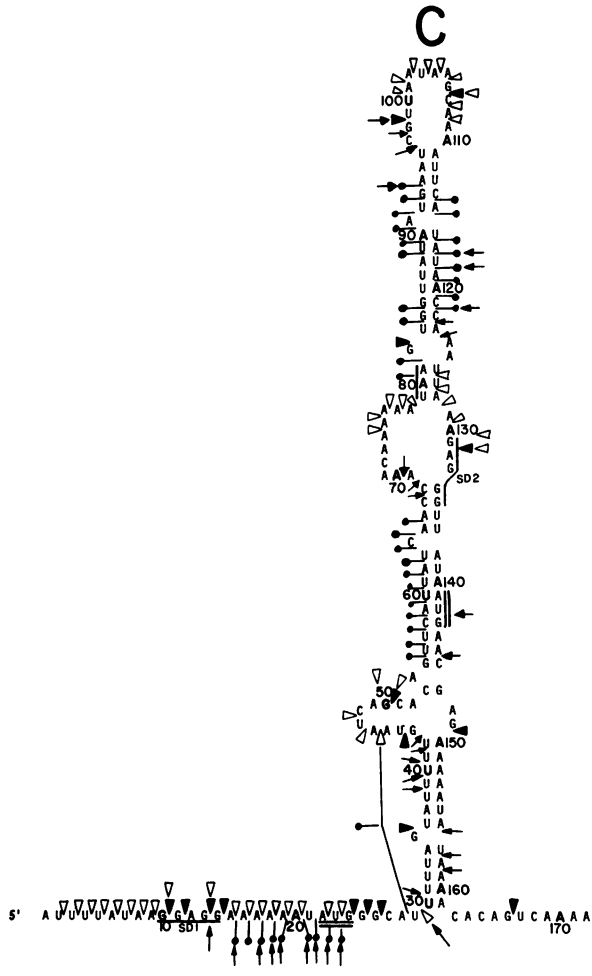

FIG. 9. Summary of the structural analysis of the ermC transcript. The cleavage patterns observed in the experiments are marked on structure C. Open triangles refer to MBN sensitive positions. Closed triangles are G residues sensitive to T1 nuclease. Lines with closed circles refer to the positions sensitive to MPE·Fe(II) and arrows refer to the positions cleaved by CVR.

The structure probing experiments, summarized in Fig. 9, also support the translational attenuation model. SD1 is shown to be essentially single-stranded, although transient base pairing of the A and U residues at positions 15-23 may occur, possibly with the A and U residues at positions 30-42. G134, G135, and G143, which occur within SD2 and the initiation codon of the rRNA methylase, are not cleaved by T1 nuclease. Likewise, U142 is clearly CVR

sensitive. The latter residue is also within the methylase initiation codon. These results are in accord with the model and with the failure of ribosomes to protect residues in the neighborhood of SD2.

The structure probing results are in accord with the main features of both structures B and C (Fig. 1), although they cannot clearly discriminate between these structures. However, as mentioned above, both structures are compatible with the regulation model for ermC. Recently, using the Zuker-Stiegler RNA folding program (30), we have obtained confirmation that structure C is the favored equilibrium structure.

ACKNOWLEDGMENT

We thank J. N. Vournakis for his generous gift of cobra venom nuclease and for his advice with the structure probing experiments. We are grateful to J.S. Krakow for generously providing RNA polymerase, to P. Dervan for his kind gift of MPE, and to R.A. Zimmerman for discussions. We thank A. Howard for expert secretarial assistance. This work was supported by grants from the National Institutes of Health.

REFERENCES

1. Pestka, S. (1977) in Molecular Mechanisms of Protein Biosynthesis, Weissbach, H. and Pestka, S., Eds., pp. 476-553, Academic Press, New York
2. Shivakumar, A.G., Hahn, J. and Dubnau, D. (1979) Plasmid 2, 279-289
3. Shivakumar, A.G. and Dubnau, D. (1981) Nucleic Acids Res. 9, 2549-2562
3a. Iordanescu, S. (1976) Arch. Roum. Path. Exp. Microbiol. 35, 111-118
4. Weisblum, B., Graham, M.Y., Gryczan, T. and Dubnau, D. (1979) J. Bacteriol. 137, 635-643
5. Shivakumar, A.G., Hahn, J., Grandi, G., Kozlov, Y. and Dubnau, D. (1980) Proc. Natl. Acad. Sci. USA 77, 3903-3907
6. Lai, C.J. and Weisblum, B. (1971) Proc. Natl. Acad. Sci. USA 68, 856-860
7. Lai, C.J., Dahlberg, J.E. and Weisblum, B. (1973) Biochemistry 12, 457-460
8. Lai, C.J., Weisblum, B., Fahnestock, S.R. and Nomura, M. (1973) J. Mol. Biol. 74, 67-72
9. Gryczan, T.J., Grandi, G., Hahn, J., Grandi, R. and Dubnau, D. (1980) Nucleic Acids Res. 8, 6081-6097
10. Horinouchi, S. and Weisblum, B. (1980) Proc. Natl. Acad. Sci. USA 77, 7079-7083.
11. Shine, J. and Dalgarno, L. (1974) Proc. Natl. Acad. Sci. USA 71, 1342-1346
12. Salser, W. (1977) Cold Spring Harbor Symp. Quant. Biol. 42(2), 985-1002
13. Cech, T.R., Tanner, N., Tinoco, Jr., I., Weir, B.R., Zuker, M., and Perlman, P.S. (1983) Proc. Natl. Acad. Sci. USA 80, 3903-3907
14. Hahn, J., Grandi, G., Gryczan, T.J., and Dubnau, D. (1982) Mol. Gen. Genet. 186, 204-216
15. Horinouchi, S. and Weisblum, B. (1981) Mol. Gen. Genet. 182, 341-348
16. Dubnau, D. (1985) EMBO J. 4, 533-537.
17. Gryczan, T.J., Contente, S. and Dubnau, D. (1978) J. Bacteriol. 134, 318-329
18. Vournakis, J.N., Celantano, J., Finn, M., Lockard, R.E., Mitra, T., Pavlakis, G., Troutt, A., van den Berg, M. and Wurst, R.M. (1981) in Gene Amplification and Analysis, Chirikjian, J. and Papas, T., Eds., Vol. 2, pp. 267-298, Elsevier-North Holland Pub. Co., New York.
19. Guha, S. and Szulmajster, J. (1974) FEBS Lett. 38, 315-319

20. Steitz, J.A. (1973) J. Mol. Biol. 73, 1-16
21. Diamond, A. and Dudock, B. (1983) Methods Enzymol. 100, 431-453
22. Vary, C.V. and Vournakis, J.N. (1984) Proc. Natl. Acad. Sci. USA 81, 6978-6982
23. Aiba, H. (1983) Cell 32, 141-149
24. Carbon, P., Ehresmann, C., Ehresmann, B. and Ebel, J.P. (1978) FEBS Lett. 94, 152-156
25. McLaughlin, J.R., Murray, C.L. and Rabinowitz, J.C. (1981) Proc. Natl. Acad. Sci. USA 78, 4912-4916
26. Steitz, J.A. (1979) in Biological Regulation and Development, Goldberger, R.F., Ed., Vol. 1, pp. 349-399, Plenum Press, New York
27. Tamm, J. and Polisky, B. (1983) Nucleic Acids Res. 11, 6381-6397
28. Hertzberg, R.P. and Dervan, P.B. (1982) J. Am. Chem. Soc. 104, 313-315
29. Loughney, K., Lund, E. and Dahlberg, J.E. (1982) Nucleic Acids Res. 10, 1607-1624
30. Zuker, M. and Stiegler, P. (1981) Nucleic Acids Res. 9, 133-148